

# Mathematical Model for Cold Rolling and Temper Rolling Process of Thin Steel Strip

Won-Ho Lee\*

*Instrumentation & Control Research Group, Technical Research Laboratories,  
POSCO, Kyungbuk 790-785, Korea*

A mathematical model for cold rolling and temper rolling process of thin steel strip has been developed using the influence function method. By solving the equations describing roll gap phenomena in a unique procedure and considering more influence factors, the model offers significant improvements in accuracy, robustness and generality of the solution for the thin strip cold and temper rolling conditions. The relationship between the shape of the roll profile and the roll force is also discussed. Calculation results show that any change increasing the roll force may result in or enlarge the central flat region in the deformation zone. Applied to the temper rolling process, the model can well predict not only the rolling load but also the large forward slip. Therefore, the measured forward slip, together with the measured roll force, was used to calibrate the model. The model was installed in the setup computer of a temper rolling mill to make parallel setup calculations. The calculation results show good agreement with the measured data and the validity and precision of the model are proven.

**Key Words :** Steel Cold Rolling, Mathematical Model, Roll Force

## 1. Introduction

Severe cases of strip rolling, such as thin strip cold rolling and temper rolling etc., cause well known problems with simplified classic circular arc models. They may have convergence difficulties or bad sensitivity to process parameters. In order to solve these problems, some researchers have attempted to develop more realistic models by the use of influence functions describing the roll deformation (Jortner et al., 1960; Grimble et al., 1976). These models gave some prediction improvement, but they failed to converge for thinner or harder materials as ever.

A major development in modeling of the thin strip and foil rolling process with the influence

function method was achieved by Fleck et al. (1992). Through assuming that there is a region of roll flattening where the roll surface is flat and parallel, they solved the non-convergence problems. In the flat region, no further reduction takes place and the shear or frictional stresses at the roll/strip interface remain at values below that predicted by the Coulomb friction law. Therefore, the roll pressure in this region can be obtained by inverting the roll profile to roll pressure relationship defined by the roll deformation influence function.

This model has provided useful reference results, however it has several shortcomings:

(1) The strip elastic deformation zones at the entry and exit were neglected, which results in an underestimation of the load. Because of the 'elastic plug'(Zhu, 1984) effect, the predicted load by this model may be much lower than the actual one. Besides, the model could not be used in light reduction rolling process in which there are relatively large entry and exit elastic zones.

(2) The pressure profile iterative loop was

---

\* E-mail : leogyber@posco.co.kr  
TEL : +82-54-220-6315; FAX : +82-54-220-6914  
Instrumentation & Control Research Group, Technical  
Research Laboratories, POSCO, Kyungbuk 790-785,  
Korea. (Manuscript Received December 5, 2001;  
Revised June 25, 2002)

taken as the basic iterative loop. The boundaries of different zones are determined with an extra iterative loop. Under some circumstances, it is very difficult to determine the boundaries of different zones (Yuen et al., 1996) because the iterative processes to determine the boundaries would diverge or not converge to unique values.

(3) The solution procedure was divided into three regimes, namely, Regime I (with no central flat zone), Regime II (with a small central flat zone and one pressure peak) and Regime III (with a large central flat zone and two pressure peaks). For the different regimes there are different algorithms. Before using the model to calculate a certain rolling case, we have to decide which regime the certain rolling case belongs to.

Although the boundaries between the different regimes were given through multi-variable regression analysis in the foil rolling case (Fleck et al., 1992), it can not be applied to other cases.

Several applications of Fleck's work were followed by Domanti et al. (1994), Dixon et al. (1995), Gratacos et al. (1994), Montmitonnet et al. (1993), Haeseling et al. (1998), and Liu et al. (2001).

Some improvements were made, but the above mentioned problems remained unsolved.

In this paper, the aforementioned shortcomings are eliminated. The strip elastic deformation at the entry and is was taken into consideration. The roll profile iterative loop is taken as the basic loop, so that the boundaries of different zones can be directly determined according to the roll profile. The extra boundary determination iterative loop is eliminated, and it is relatively easy to determine the boundaries of the different zones. Besides, which regime the rolling case belongs to can also be directly determined by observing the shape of the roll profile. Therefore, it would not be necessary to determine the regimes and choose the calculation procedure before hand.

After calibration using the production data, the newly developed model is applied to the actual temper rolling process and the validity and precision of the model are also proven.

## 2. Main Equations

A geometric sketch of the deformation zones is shown in Fig. 1. The geometric parameters are defined with a polar coordinates system.

The roll-gap model is based on two relationships which enable a gauge profile to be calculated from a known pressure profile and conversely a pressure profile to be calculated from a gauge profile.

The elastic deformation of the work roll is related to the roll pressure via the linear integral equation.

$$a(\theta) = \int_0^\theta U(\theta-t)p(t)dt + R \quad (1)$$

where  $a(\theta)$  : work roll radius at point  $\theta$ ;

$R$  : undeformed radius of work roll;

$p(t)$  : pressure profile.

$U(\theta-t)$  : Jortner's influence function [9, 10];

$$U(\theta-t) = \frac{R\Delta\theta}{\pi E} \left\{ (1-\nu^2) \left[ \cos(\theta-t) \ln \left( \frac{1-\cos(\theta-t)}{1+\cos(\theta-t)} \right) + 2 \right] - (1-\nu-2\nu^2) \sin^2(\theta-t) \left[ \tan^{-1} \left( \frac{1+\cos(\theta-t)}{\sin(\theta-t)} \right) + \tan^{-1} \left( \frac{1-\cos(\theta-t)}{\sin(\theta-t)} \right) \right] \right\} \quad (2)$$

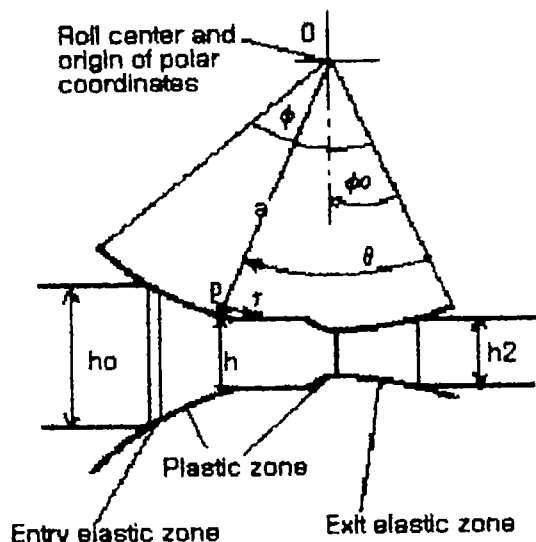


Fig. 1 Sketch of the deformation zones in the roll gap

where  $\Delta\Phi$  : segmental angle ;

The gauge profile is determined by the deformed roll radius according to the equation.

$$h(\theta) = R_s - 2a(\theta) \cos(\theta - \phi_0) \quad (3)$$

where  $h(\theta)$  : gauge profile ;

$R_s$  : distance between centers of the work rolls ;

$\Phi_0$  : angle measured to the line of work roll centers.

The pressure profile is related to the gauge profile via differential equations. In the entry and exit elastic regions it is :

$$\frac{dp}{d\theta} = -\frac{2a}{h} \left[ \frac{\mu p v + p(1-2v) \tan\beta}{1-v} + \frac{(2h-h_1) \tan\beta E}{h_1(1-v^2)} \right] \quad (4)$$

and in the plastic regions :

$$\frac{dp}{d\theta} = -\frac{2a}{h} (\mu p - y \tan\beta) + \frac{dy}{d\theta} \quad (5)$$

where  $v$  : Poisson's ratio ;

$E$  : Young's modulus of elasticity ;

$h_1$  : unstrained gauge in a elastic region ;

$\beta$  : angle between deformed roll and horizontal ;

$y$  : yield stress ;

$\mu$  : friction coefficient between rolls and the strip ;

In the central flat region, the discrete pressure profile can be obtained by solving the following linear equation system (all parameters are expressed in discrete form) :

$$\sum_{j=1}^{j_1} (U_{e,j} - U_{e,j}) p_j = \frac{R_s - h_i}{2 \cos(\theta_i - \Phi_0)} - \frac{R_s - h_e}{2 \cos(\theta_e - \Phi_0)} \quad (6)$$

$$-\sum_{j=1}^{j_1} (U_{e,j} - U_{e,j}) p_j + \sum_{j=1}^{j_2} (U_{e,j} - U_{e,j}) p_j \quad i=j_1, \dots, j_2$$

where  $j_1$  : the first node in the flattened region ;

$j_2$  : the final node in the flattened region ;

$e$  : the node at entry plane ;

$d$  : the node at exit plane.

Once the pressure and gauge profiles are determined, the roll force,  $P$ , and torque,  $T$ , can be calculated through integration of the pressure and friction force distribution :

$$P = \int_0^\pi a(\theta) \frac{\cos\beta}{\cos\xi} [p(\theta) + \tau(\theta) \tan\beta] d\theta \quad (7)$$

$$T = \int_0^\pi a^2(\theta) [\tau(\theta) + p(\theta) \tan\xi] d\theta \quad (8)$$

where  $\xi$  : angle between undeformed roll and horizontal axis.

At the same time, the forward slip,  $f$ , can also be approximately calculated with the following formula :

$$f = h_n/h_2 - 1 \quad (9)$$

where  $h_n$  : strip gauge at a flat region or a neutral point ;

$h_2$  : strip gauge at the exit side.

### 3. Calculation Procedure and Analysis of New Model

The main flow chart of the calculation procedure is shown in Fig. 2. The iterative calculation procedure is introduced to solve the equations describing the roll-deformation and the strip-stress distribution. No matter which regimes the

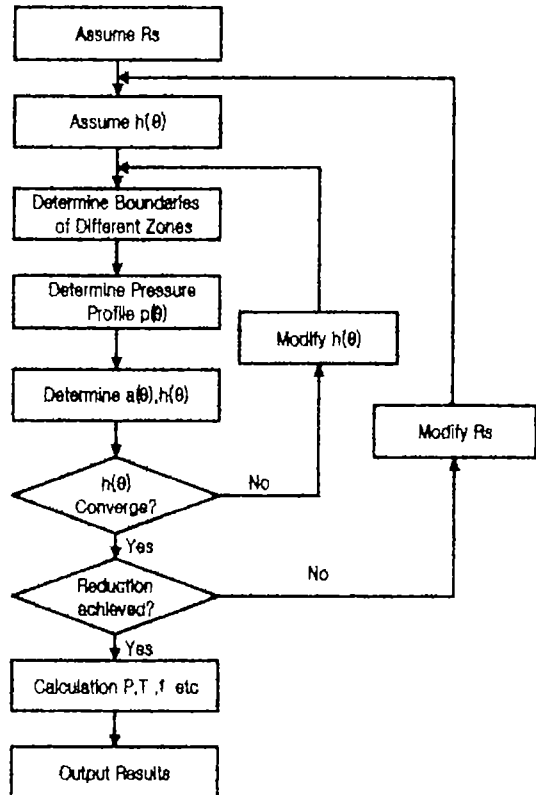


Fig. 2 The calculation procedure of new model

rolling conditions belong to, the same calculation procedure can be used. That is one of the most important advantages in the present model.

Before applying the present model to actual temper rolling process, the reliability and convergence of calculation result were checked with various rolling conditions. Here, some typical calculated results are introduced.

Figure 3 is an example of foil, which is ultra thin material, cold rolling process calculation. Three reduction rates were used in the calculation

Though very thin entry thickness was used, there was no convergence problem, in this model.

It can be seen that as the reduction increases from 50% to 70%, the pressure profile changes

from one peak (regime II) to two peaks (regime III), and the length of the flat region and the roll force also increases more than two times. It reveals that the same calculation procedure can be used regardless of deformation regimes in the present model.

Figure 4 shows the effect of the friction coefficient upon the gauge and pressure profile under temper rolling conditions. It can be seen that not only the pressure profile but also the gauge profile is greatly influenced by the friction coefficient. At low friction conditions, the contact arc between the roll and the strip is nearly circular, but at high friction conditions, a flat region appears in the central part of the contact arc.

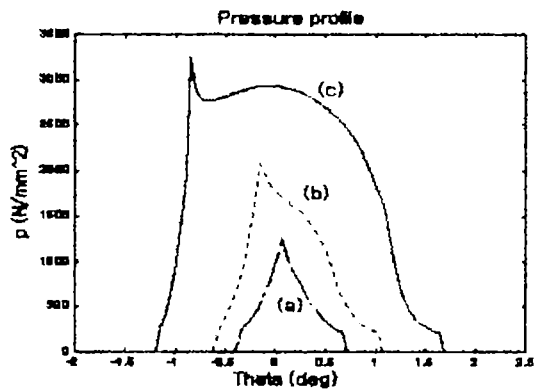
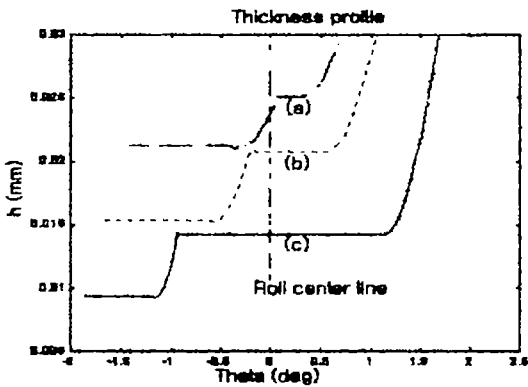


Fig. 3 Thickness and pressure profile of foil cold rolling

$R=89$  mm, friction coefficient=0.03,  $\sigma_y=230$  Mpa, entry thickness=0.03 mm,  $E=230$  Gpa,  
 (a) reduction=30%, (b) reduction=50%, (c) reduction=70%

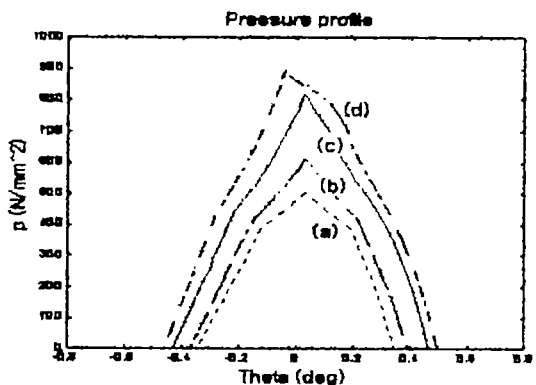
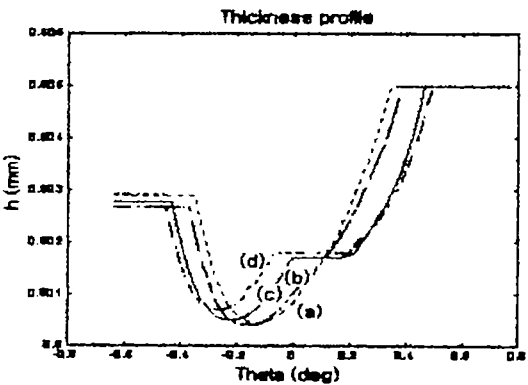
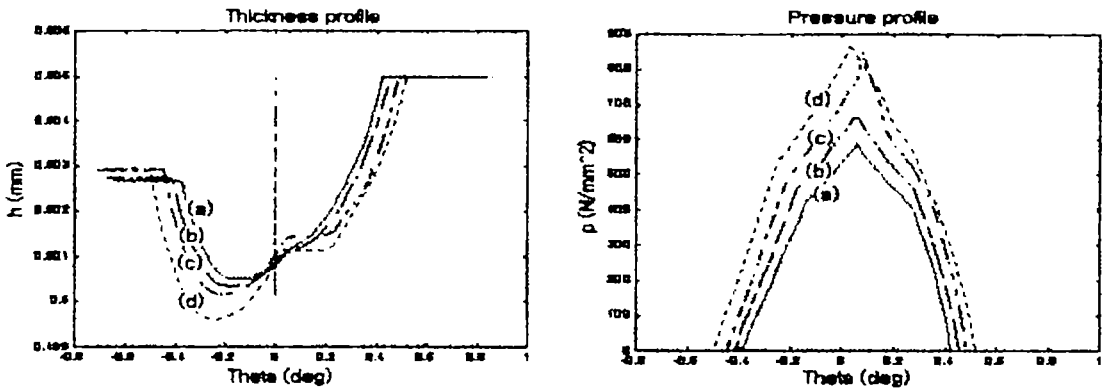


Fig. 4 Thickness and pressure profile under different friction coefficients

$R=205$  mm,  $\sigma_y=196$  Mpa, entry thickness=0.505 mm, reduction=0.46%, rolling speed=37 m/min,  
 entry tension=2496 kg, exit tension=3616 kg, width=1073 mm,  
 (a)  $\mu=0.12$ , (b)  $\mu=0.15$ , (c)  $\mu=0.18$ , (d)  $\mu=0.21$



**Fig. 5** Thickness and pressure profile under different yield stress  
 $R=205$  mm, entry thickness=0.505 mm, reduction=0.46%, width=1073 mm, rolling speed=37 m/min, entry tension=2496 kg, exit tension=3616 kg,  $\mu=0.12$   
 (a)  $\sigma_y=210$  MPa, (b)  $\sigma_y=240$  MPa (c)  $\sigma_y=270$  MPa, (d)  $\sigma_y=300$  MPa

Similar situation can also be seen when we change the yield stress of the strip. As shown in Fig. 5, the contact arc changes its shape from nearly circular to non-circular, and a central flat region finally appears, as the yield stress increases. Besides, the elastic recover zone is also greatly influenced by the yield stress.

Through the analysis of rolling phenomena, it was confirmed that the new model has a calculation stability and can give physically reasonable result for wide range of temper rolling conditions.

#### 4. Model Calibration and Application Result

In order to use the theoretical model as a setup model in the elongation control system of a temper rolling mill in POSCO, the model was calibrated against the production data collected from the same mill. The friction coefficient,  $\mu$  and the constrained yield stress,  $K$ , were taken as the calibration factors. Because the roll force,  $P$ , and the forward slip,  $f$ , can be measured in the temper rolling mill, and they can also be calculated by the theoretical model, we used these two measured data to determine the calibration factors  $K$  and  $\mu$ . Equating the measured roll force  $P_m$  and forward slip  $f_m$  with their calculation formula, which were derived from the theoretical model,

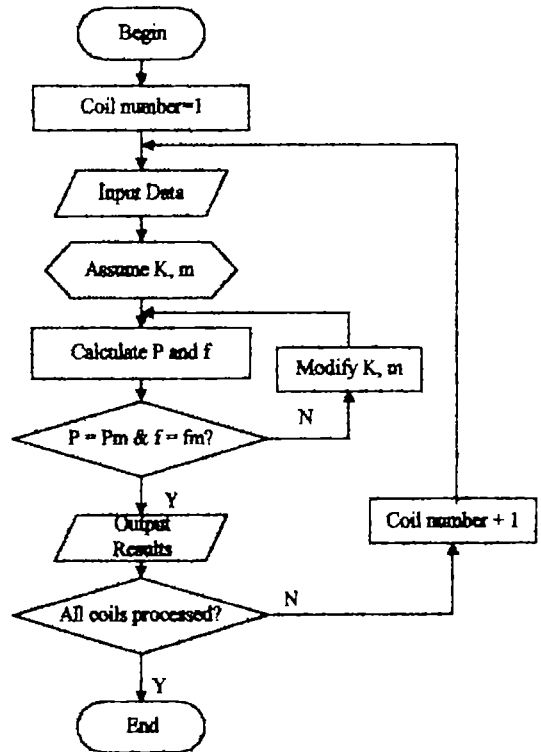


**Fig. 6** Calculation of constrained yield stress and friction coefficients

we got two coupled equations. Solving the coupled equations with the iterative method, we obtained the constrained yield stress,  $K$ , and the friction coefficient  $\mu$  for each coil.

Because present model can well predict the

**Table 1** The values of the calibration factors for each group

Steel group	Constrained yield stress (N/mm <sup>2</sup> )	Friction coefficient
C1CS	271.3	0.1275
CCCS	280.1	0.1262
CHR35R	201.9	0.1373
CH40R	237.8	0.1200
CDCS	168.3	0.1235
CNCS	163.9	0.1251
CECS	155.4	0.277
CVE1	178.5	0.1141
Mn60	276.7	0.1251
CH35E	160.9	0.1256
CT37	255.5	0.1527
CC8H	313.9	0.1214
CH60C	418.6	0.1157
CX80DP	421.7	0.1688

large forward slip in the temper rolling process, we got reasonable results using the above method. A flow chart of the calibration calculation is shown in Fig. 6.

After the constrained yield stress and friction coefficients were calculated for all coils, we divided the coils into groups according to the steel grades and the constrained yield stress. The average constrained yield stress and average friction coefficient of each group were used as the final values of the calibration factors for this group. Table 1 shows the values of the calibration factors for each group.

After calibration, the model was installed in the plant together with the data acquisition system to make parallel calculations and comparisons. An evaluation sample that consists of the valid data of 3724 coils is adopted to make the evaluation and comparison.

Figure 7 shows comparison of the measured roll forces and the roll forces calculated by a present model. It can be seen that the predicted roll forces match the measured values well and the model has relatively high prediction accuracy. A statistical analysis shows that the correlation coefficient between the measured roll forces and

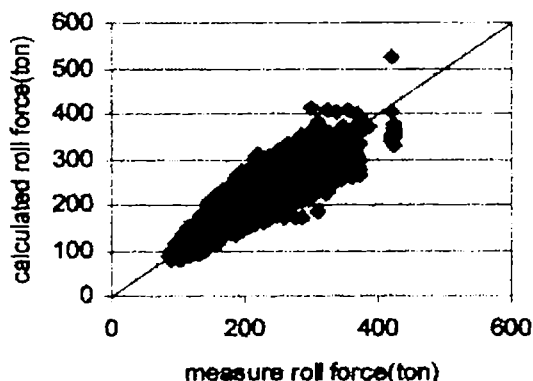


**Fig. 7** Roll force measured and predicted by the present model

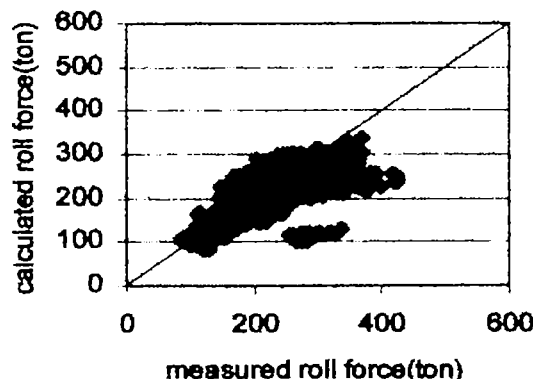


**Fig. 8** Roll force measured and predicted by the regression model

the roll forces predicted by the present model equals 0.8899.

In order to show the prediction accuracy improvement made by the present model, the regression model, which had been used as the setup model in the same temper rolling mill before the present model was developed, was also evaluated with the same data. Figure 8 shows comparison of the measured roll force and the roll force calculated by the regression setup model.

As we can see, the samples in Fig. 8 are more scattered than those in Fig. 7. The correlation coefficient between the measured roll force and the roll force calculated by the regression setup model is 0.7175. Besides, the average calculated roll force is lower than that of the measured roll force. This indicates that the regression setup model underestimated the roll force in general. By

comparison, we can see that the present theoretical model is much more accurate than the regression setup model. From a comparison with the measured data and comparison with the old setup model, the validity and precision of the present model are proven.

## 5. Conclusions

A new mathematical model for the thin strip cold and temper rolling process has been developed by modification of the influence function method. The main differences of present model against to basic influence function method are to be summarized as follows :

(1) The strip elastic deformation at the entry and exit was taken into consideration.

(2) The roll profile iterative loop was taken as the basic loop so that the boundaries of different zones can be directly determined according to the roll profile.

(3) The new calculation procedure was introduced to apply the new model to various rolling conditions. Therefore, it would not be necessary to determine the regimes and choose the calculation procedure before hand.

By solving the equations describing the roll gap phenomena in a unique procedure, the new model offered significant improvement in the accuracy, robustness and generality of the solution for thin strip cold and temper rolling conditions.

The model was installed in the process computer of an actual temper rolling mill to make setup calculations. The calculation results showed good agreement with the measured data and the validity and precision of the model were proven.

## References

- Dixon, A. E. and Yuen, W. Y. D., 1995, "A Computationally Fast Method to Model Thin Strip Rolling," *Proc. Computational Techniques and Applications Conference 95*, Melbourne, Australia, July 3-5, pp. 239~246.
- Domanti, S. A., Edwards, W. J., Thomas, P. J. and Chefneux, I. L., 1994, "Application of Foil Rolling Models to Thin Steel Strip and Temper Rolling," *Proc. 6th International Rolling Conference*, Duesseldorf, Germany, June 20-22, pp. 422~429.
- Fleck, N. A., Johnson, K. L., Mear, M. E. and Zhang, L. C., 1992, "Cold Rolling of Foil," *Proc. Inst. Mech. Eng., Part B: J. Eng. Man.*, Vol. 206, pp. 119~131.
- Gratacos, P. and Onno, F., 1994, "Elastoplastic Models for Cold Rolling, Application to Temper Rolling," *Proc. 6th International Rolling Conference*, Duesseldorf, Germany, June 20-22, pp. 441~445.
- Grimble, M. J., 1976, "A Roll Force Model for Tinplate Rolling," *GEJ. of Science & Tech.*, Vol. 43, No. 1, pp. 3~12.
- Haeseling, G., Kastner, S., Kramer, A. and Hartung, H. G., 1998, "New Foil Rolling Theories and Their Importance for Industrial Practice," *MPT International*, No. 6, pp. 86~91.
- Jortner, D., Osterle, J. F. and Zorowski, C. F., 1960, "An Analysis of Cold Strip Rolling," *Int. J. Mech. Sci.*, Vol. 2, pp. 179~194.
- Liu, Y. and Lee, W., 2001, "Application of the Preliminary Displacement Principle to the Temper Rolling Model," *KSME International Journal*, Vol. 15, No. 2, pp. 225~231.
- Montmitonnet, P., Massoni, E., Vacance, M., Sola, G. and Gratacos, P., 1993, "Modeling for Geometrical Control in Cold and Hot Rolling," *Ironmaking and Steelmaking*, Vol. 20, No. 4, pp. 254~260.
- Yuen, W. Y. D., Nguyen, D. N. and Matthews, D. L. 1996, "Mathematical Modeling of the Temper Rolling Processes," *37TH MWSP CONF. PROC.*, ISS, Vol. XXXIII, Ontario Canada, pp. 165~172.
- Zhu, Q., 1984, "Deformation Characteristics of the Cross Shear Cold Rolling of Ultra Thin Strip and the Theory of 'Elastic Plug'," *Proc. Adv. Technol. Plastic.*, Vol. 2, p. 1173.